Observation of the Transition from Thomson to Compton Scattering in Multiphoton Interactions with Low-Energy Electrons

C. I. Moore, J. P. Knauer, and D. D. Meyerhofer

Laboratory for Laser Energetics, University of Rochester, 250 East River Road, Rochester, New York 14623-1299
(Received 1 August 1994)

We have observed longitudinal acceleration of free electrons by photon scattering in the low-energy Thomson regime. This is the first observation of the transition between the Thomson and Compton regimes of electron scattering due to higher-order photon interactions.

PACS numbers: 32.80.Rm, 42.50.Vk

The usual distinction between the Thomson and Compton scattering regimes for free electrons is the energy of the incident photon. Thomson scattering is the low-energy limit of Compton scattering, in the regime where the photon energy $\hbar\omega$ is much less than the electron rest energy mc^2. This condition is satisfied by 5 orders of magnitude for optical photons. As the photon energy approaches mc^2, the scattering process becomes affected by the relativistic considerations of the Compton process. However, more than 30 years ago it was predicted on both quantum mechanical [1–5] and classical [6] grounds that the border between the Thomson and Compton regimes could be crossed without raising the photon energy if enough photons could be absorbed coherently, i.e., in a time short compared to the time the electron can be expected to undergo a collision with another electron or be captured by an ambient ion. This was the second multiphoton effect predicted for free electrons, after the Kapitza-Dirac prediction [7] in 1933 of stimulated Compton scattering. This was observed recently by Bucksbaum, Schumacher, and Bashkansky [8] in the Thomson regime. A variety of multiphoton effects, including parity-forbidden, even-order harmonic generation, has been predicted for free electrons crossing the Thomson-Compton border with the aid of an intense photon field [5,9,10]. The observation of even-harmonic generation has not yet been reported.

The "border-crossing" effects are difficult to observe because they require an electron to be immersed in a dense cloud of photons. Electrons incident from outside the laser focus can be scattered by the ponderomotive potential of the focus before they reach the high-intensity region. This was observed at low energies by Bucksbaum, Bashkansky, and McIlrath [11]. If the electrons are produced externally and then enter and leave the high-density photon bath (laser focus) smoothly, dressing effects are built up upon entry and then left behind upon departure. We have been able to overcome this difficulty by observing the electron-photon scattering of low-energy electrons that have been produced in the intense region of the laser focus by field ionization [12]. The development of short-pulse, high-intensity, tabletop lasers [13] has allowed high-intensity interactions to be observed on time scales short compared to the typical collision times.

This Letter reports the first observation of a forward electron momentum due to the nonlinear scattering of low-energy free electrons with an intense electromagnetic wave. Neon densities of 3×10^{13} cm^{-3} were used as a source of electrons for this experiment. The forward ($\mathbf{k}$) drift (acceleration) is a consequence of the conservation of photon energy and momentum in the interaction of the field with a single electron (Compton scattering). The low density of the interaction gas ensures that this is not a collective or plasma effect and that the interaction time is much shorter than the collision time, ensuring full coherence of the free electron scattering events of interest.

The observed longitudinal momentum of an electron arises from the absorbed longitudinal momentum p_z, which accompanies the energy absorbed from the focused laser field [14]. For an electron that is born at rest in the laser field, the energy absorbed from the field ΔE and the longitudinal momentum are related by $cp_z = \Delta E = (\gamma - 1)mc^2$, where $E = \gamma mc^2$ is the total electron energy. The total electron momentum is

$$|\mathbf{p}|^2 = \frac{E^2}{c^2} - m^2c^2 = (\gamma^2 - 1)m^2c^2. \tag{1}$$

The electrons leave the laser focus at an angle θ with respect to the k vector of the laser given by

$$\theta = \cos^{-1}\sqrt{\frac{\gamma - 1}{\gamma + 1}} = \tan^{-1}\sqrt{\frac{2}{\gamma - 1}}. \tag{2}$$

The longitudinal momentum can also be calculated from the electron's trajectory in an intense electromagnetic field [1,6,10]. At very high intensities, a free electron's oscillatory motion in a laser field becomes anharmonic. The nonlinear electromagnetic wave effects can be parametrized by q (sometimes called η) [10],

$$q^2 = 2\,e^2\langle A^2\rangle/m^2c^4, \tag{3}$$

where c is the speed of light, e and m are the electron charge and rest mass, respectively, ω is the laser frequency, and $\langle A^2\rangle$ is the time average of the square of the vector potential of the laser. q is related to the ponderomotive potential (average quiver energy) of the laser by $\Phi_{\text{pond}} = q^2mc^2/4$. As q approaches 1, a significant drift

0031-9007/95/74(13)/2439(4)$06.00

arises in the direction of the laser wave vector **k**. This forward momentum is second order in q.

Free electron interactions with laser pulses where q approaches 1 were examined in our experiment. Free electrons were created via ionization in the laser focus, and the ejected electron distribution as a function of energy and angle from the beam axis was measured. The final electron energy arises from two sources, the conservation of canonical angular momentum [10,15] and the ponderomotive acceleration out of the focus [1,6]. An electron born in the focus of a laser pulse that leaves the focus in a time short compared to the laser pulse duration will have a final energy [16]

$$E(t = \infty) = \left(\frac{e\mathbf{A}(0)}{\sqrt{2mc^2}} \right)^2 + \Phi_{\mathrm{pond}} + mc^2, \qquad (4)$$

where $\mathbf{A}(0)$ is the vector potential at the time the electron is born in the laser field. For electrons born at the peak of a linearly polarized field, $\mathbf{A}(0) = 0$, whereas it is nonzero for circular polarization leading to an ejected electron kinetic energy equal to twice the ponderomotive potential [16,17]. In our experiments an electron is released via ionization into the presence of an already intense electromagnetic field. Electrons created by ionization are typically released with a few electron volts of energy [18], which can be considered to be at rest when the ponderomotive potential is much larger. Experiments by Corkum, Burnett, and Brunel [16] with $q \sim 0.01$ were consistent with this picture. The drift of the electrons is shown schematically in Fig. 1.

These results have been confirmed by a fully relativistic Monte Carlo simulation of the electron dynamics. The simulation involved propagating a circularly polarized Gaussian temporal and spatial profile laser pulse over a few thousand atoms placed at random positions within a laser focus. The parameters were based on our laser system. Electrons with zero initial velocity are released into the field at the electric field strength necessary for

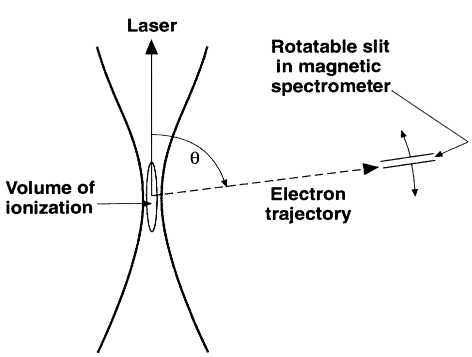

FIG. 1. Experimental setup showing the position of the magnet gap in the spectrometer in relation to the laser focus, a typical electron trajectory, and the definition of theta. The volume of ionization refers to the volume in which the intensity exceeds the threshold intensity of ionization for a particular charge state and is not to scale.

Coulomb barrier suppression ionization (BSI) [12]; $F = \varepsilon_{\mathrm{ion}}^2/4Z$ (in atomic units), where $\varepsilon_{\mathrm{ion}}$ is the ionization potential and Z is the ionic charge. The fully relativistic equation of motion for the electron trajectories was solved for each electron. These electron energies and trajectories agreed with Eqs. (2) and (4). Calculations of the initial momentum of electrons produced during the ionization of atoms in strong fields by Reiss [19] and Delone and Krainov [20] are consistent with Eq. (2).

We have constructed a magnetic spectrometer to measure the energy and angular (relative to **k**) distributions of electrons emitted from a high-intensity laser focus. The spectrometer consists of an electromagnet to select the electron energy and a detector consisting of a scintillator coupled to a photomultiplier tube (PMT).

The analyzing magnet is a 10 cm square piece of high-purity iron with a 6 cm square cut from the center. A 2 mm gap was cut in one side of the iron. A 100 ms, square-topped current pulse, fired 80 ms before the laser pulse, produces a constant magnetic field. Residual fields or hysteresis effects in the iron core of the magnet are minimized by de-Gaussing after every shot. Magnetic fields from 50 to 6000 G are reliably formed with less than 2% fluctuations from shot to shot.

The magnet is placed above the laser focus with the 2 mm gap aligned with the focus, which allows a line of sight to be traced from the focus through the gap in the magnet. Electrons emitted from the laser focus toward the gap in the magnet enter the gap and are curved by the magnetic field. Those with a gyroradius of 1.8 cm strike the scintillator where ultraviolet photons are emitted. The photon flux is then measured using the PMT, and the electrical signal is read by an analog-to-digital converter. Peak signal-to-noise ratios of 1000 to 1 are obtained.

The energy window of the spectrometer is varied by changing the magnetic field in the gap of the steering magnet. A calibration has been performed using an electron gun producing electrons of known energy. The electron gun was placed at the laser focus and aimed toward the gap in the steering magnet. The magnetic field in the gap was varied by adjusting the voltage applied across the coils of the electromagnet, allowing a measurement of the applied voltage versus electron energy. The calibration showed an energy window of $\Delta E/E \sim 0.3$ FWHM.

The angular distribution of electrons in θ (relative to **k**) is measured by rotating the entire spectrometer about the cylindrical axis that passes through the laser focus at 90° to the laser axis. The gap in the magnet is always aligned so that a clear line of sight can be traced from anywhere on this central axis through the gap in the magnet (see Fig. 1).

The angular resolution is $\pm 1.5°$; this uncertainty comes from two sources. The first is the geometric angular resolution due to the 2 mm gap in the magnet, which corresponds to an angular spread of $\pm 1°$ for electrons traveling from the laser focus. The second is due to an asymmetry in the magnetic field of the magnet in the spectrometer. A slight tilt in the magnetic field deflected electrons by $3.5° \pm 0.5°$ from their original ejection angle. This angle was determined from the detection angle of the N^{4+} electron peak on one side of the laser focus compared to its position on the opposite side of the focus. The symmetry of the focus requires that this peak occur at the same angle from the **k** on both sides of the focus. This determination is accurate to $\pm 0.5°$ and, when combined with the geometric resolving power of the gap, gives a total uncertainty in the angle of $\pm 1.5°$.

The laser system used for the experiments was a 1.053 μm, 1 ps laser using chirped-pulse amplification (CPA), which is described elsewhere [21]. The laser was focused to a 5 μm ($1/e^2$ radius) focal spot and a peak laser intensity of approximately 10^{18} W/cm^2 ($q \sim 0.7$) in neon at a pressure of 1×10^{-3} Torr. Circular polarization was used to avoid possible asymmetries in the electron angular distribution in the plane of polarization upon ionization due to nonzero initial velocities of the electrons along the electric field [16]. Helium was ionized to confirm the expected ponderomotive energies associated with the BSI threshold intensities. Ne^{3+} is created at approximately the same intensity as He^{2+} [12]. This was used to determine the electron peaks in the neon spectrum.

Observations of the energies of the electrons ionized from the 3^+ through 8^+ charge states of neon were found to be in agreement with the expected ponderomotive energies associated with their corresponding BSI threshold intensities.

Figure 2 shows the measured angular distribution of the 3^+ and 8^+ electrons of neon and their expected theoretical positions based on the Monte Carlo simulation. The angular spread in the electron distributions is due primarily to the intensity distribution of the laser focus. The ponderomotive force is linearly related to the gradient of the intensity distribution, which is not always perpendicular to the beam axis in a focused Gaussian beam. This results in some electrons having a small component of ponderomotive acceleration along the beam axis. This acceleration is symmetric about 90° to the beam axis due to the symmetry of a Gaussian beam as it passes through focus and cannot explain any forward shift of the peak of the electron distribution. The normalized electron number on the y axis is due to the lack of an absolute calibration of the detector. A single normalization constant was used in a least squares fit between Monte Carlo simulation and experimental data for all the charge states.

Figure 3 shows the angle of peak electron number for the 3^+ through 8^+ neon charge states measured as a function of the electron energy. The measurements (open circles) are in good agreement with the Monte Carlo simulation (crosses) and with the predictions of Eq. (2).

We have made the first observations of a forward acceleration of electrons in a high-intensity laser focus due to the transition from Thomson to Compton effects (relativistic quiver motion). Good agreement between the forward shifted angle of the fully relativistic theoretical predictions and the data has been obtained.

The authors gratefully acknowledge conversations with J. H. Eberly and M. V. Fedorov. This work was supported by the U.S. Department of Energy Office of Basic Energy Sciences, Division of Chemical Sciences. Additional support was provided by the U.S. Department of Energy Office of Inertial Confinement Fusion under Cooperative Agreement No. DE-FC03-92SF19460, the University of Rochester, and the New York State Energy Research and Development Authority.

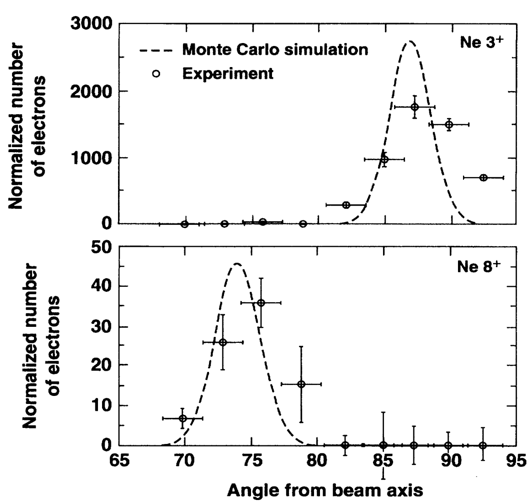

FIG. 2. Observed experimental angular distribution data points for electrons born during the production of the 3^+ and 8^+ charge states of neon. The dashed curves represent the expected angular distribution for each charge state from the theoretical Monte Carlo simulation of the electron dynamics.

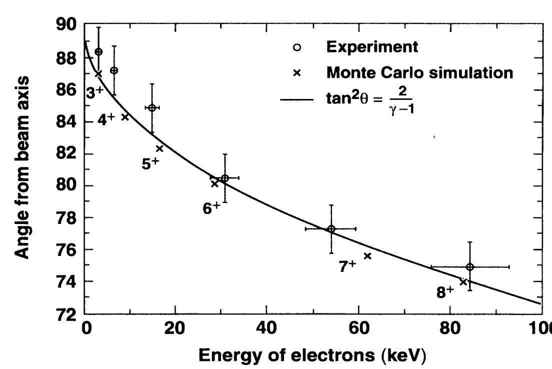

FIG. 3. Angle of peak electron number versus kinetic energy for electrons born during the production of the 3^+ through 8^+ charge states of neon from the experiments (○) and the Monte Carlo simulation (×). The solid curve is the theoretical prediction of Eq. (3).

[1] L. S. Brown and T. W. B. Kibble, Phys. Rev. **133**, A705 (1964).
[2] O. von Roos, Phys. Rev. **135**, A43 (1964).
[3] Z. Fried and J. H. Eberly, Phys. Rev. **136**, B871 (1964).
[4] T. W. B. Kibble, Phys. Rev. **150**, 1060 (1966).
[5] J. H. Eberly in *Progress in Optics,* edited by E. Wolf (North-Holland, Amsterdam, 1969), Vol. 7.
[6] J. H. Eberly and A. Sleeper, Phys. Rev. **176**, 1570 (1968).
[7] P. L. Kapitza and P. A. M. Dirac, Proc. Cambridge Philos. Soc. **29**, 297 (1933).
[8] P. H. Bucksbaum, D. W. Schumacher, and M. Bashkansky, Phys. Rev. Lett. **61**, 1182 (1988).
[9] Vachaspati, Phys. Rev. **128**, 664 (1962).
[10] E. S. Sarachik and G. T. Schappert, Phys. Rev. D **1**, 2738 (1970).
[11] P. H. Bucksbaum, M. Bashkansky, and T. J. McIlrath, Phys. Rev. Lett. **58**, 349 (1987).
[12] S. Augst, D. Strickland, D. D. Meyerhofer, S. L. Chin, and J. H. Eberly, Phys. Rev. Lett. **63**, 2212 (1989).
[13] P. Maine, D. Strickland, P. Bado, M. Pessot, and G. Mourou, IEEE J. Quantum Electron. **24**, 398 (1988).
[14] P. B. Corkum, N. H. Burnett, and F. Brunel, in *Atoms in Intense Laser Fields,* edited by M. Gavrila (Academic Press, New York, 1992), pp. 109–137.
[15] W. B. Mori and T. Katsouleas, Phys. Rev. Lett. **69**, 3495 (1992).
[16] P. B. Corkum, N. H. Burnett, and F. Brunel, Phys. Rev. Lett. **62**, 1259 (1989).
[17] P. H. Bucksbaum, L. D. Van Woerkom, R. R. Freeman, and D. W. Schumacher, Phys. Rev. A **41**, 4119 (1990).
[18] R. R. Freeman and P. H. Bucksbaum, J. Phys. B **24**, 325 (1991).
[19] H. R. Reiss, J. Opt. Soc. Am. B **7**, 574 (1990).
[20] N. B. Delone and V. P. Krainov, J. Opt. Soc. Am. B **8**, 1207 (1991).
[21] Y.-H. Chuang, D. D. Meyerhofer, S. Augst, H. Chen, J. Peatross, and S. Uchida, J. Opt. Soc. Am. B **8**, 1226 (1991).